Investigation of Thermionic Emission in the Region of Periodic Schottky Deviation

JAN-JAN YANG AND TIEN-TSAI YANG
University of California, Los Angeles, California 90024
(Received 7 August 1969)

The existence of deviation from the thermionic Schottky line has been theoretically investigated for metals. An equation based on a modified model, which contains a classical image force and exchange and correlation forces, is derived. The theoretical solution indicates that the amplitude is inversely proportional to the temperature, whereas the phase and the period are found to be independent of the temperature. The theoretical solution is compared with the experiments in terms of two parameters, the potential-barrier height and the coefficient of the exchange and correlation forces. These exchange and correlation forces characterize the form of the surface potential. The agreement in amplitude and phase between theoretical and experimental results is excellent.

I. INTRODUCTION

THE periodic deviation from the Schottky line in thermionic emission was explained by Guth and Mullin[1] as resulting from the interference between electron waves reflected from the barrier maximum and those reflected from a region of steep potential gradient near the surface of the metal. Guth and Mullin[1] derived a periodic transmission coefficient by using the free-electron model of a metal and a one-dimensional classical image potential, and found a good agreement in period with the experimental results of Siefert and Phipps.[2,3] However, their amplitude and phase of periodicity did not agree with the experimental results. The theory was modified in terms of a revised transmission coefficient, defined by Herring and Nichols,[4] by Juenker, Colladay, and Coomes,[5] Juenker,[6] and Miller and Good.[7] Their results gave the correct period for the deviations and also agreed with the observed variation of the amplitude with field and temperature. However, quantitatively, the observed amplitudes and phases of the deviations did not agree with the theory. A possible source of the disagreement might have been the validity of the WKB approximation used in both the original Guth-Mullin theory and in Juenker *et al.* Miller and Good,[8] however, making use of the more exact WKB-type approximation in recalculatlng the periodic deviations, obtained essentially the same results as in Juenker *et al.* Since they used the same model as Juenker *et al.*, the agreement removes any uncertainty about the mathematical approximation.

Cutler and Gibbons[9] developed a model for the surface potential barrier based on the quantum-mechanical calculation made by Bardeen[10] and the form of the potential at the surface of a sodiumlike metal and the analysis of Sachs and Dexter[11] on the quantum limits of the image-force theory. Employing this model, the periodic deviations were recalculated using essentially the mathematical formalism developed by Juenker[6] and his co-workers. Certain computational refinements were introduced in the averaging of the transmission coefficient. The results were found to be in better agreement with the experimental data in the phase of periodic deviations than others. However, the amplitudes and phases are still not in agreement with the experimental observations.

A possible origin of this disagreement lies in the use of the free-electron model by assuming

$$W_a = E_F + \theta,$$
$$= (\hbar^2/2m)(3\pi^2/V)^{2/3} + \theta,$$

where W_a is the barrier-height difference between the inside and outside of the metal surface, E_F is the Fermi energy, θ is a work function, $\hbar$ $(=h/2\pi)$ is Plank's constant, m is the mass of the electron, and V is the atomic volume.

The values of W_a for tungsten, tantalum, and molybdenum so obtained are almost the same, i.e., it is about 10 eV. According to the theory, the periodicity from the Schottky line for these metals should be about the same. However, there is a considerable difference in the experimental results.

From the energy-band structure of tungsten and rhenium, W_a is assumed to be the summation of the work function and the difference between the Fermi energy and the bottom of conduction band, i.e., $W_a = \theta + (E_F - E_c)$. From Mattheiss's calculations,[12,13] the values of W_a for tungsten and rhenium found by this way are 6.1 and 7.4 eV, respectively.

In the present analysis (1) a modified model of potential barrier has been developed by considering not only classical image force and the external force but also the exchange and correlation forces; and (2) the values of W_a for tungsten and rhenium obtained from the

[1] E. Guth and C. J. Mullin, Phys. Rev. **59**, 575 (1941).
[2] R. L. E. Seifert and T. E. Phipps, Phys. Rev. **53**, 493 (1938).
[3] R. L. E. Seifert and T. E. Phipps, Phys. Rev. **56**, 652 (1939).
[4] C. Herring and M. H. Nichols, Rev. Mod. Phys. **21**, 185 (1949).
[5] D. W. Juenker, G. S. Colladay, and E. A. Coomes, Phys. Rev. **90**, 772 (1953).
[6] D. W. Juenker, Phys. Rev. **99**, 1155 (1955).
[7] S. C. Miller and R. H. Good, Jr., Phys. Rev. **92**, 1367 (1953).
[8] S. C. Miller and R. H. Good, Jr., Phys. Rev. **91**, 174 (1953).
[9] P. H. Cutler and J. J. Gibbons, Phys. Rev. **111**, 394 (1958).
[10] J. Bardeen, Phys. Rev. **49**, 653 (1936).
[11] R. G. Sachs and D. L. Dexter, J. Appl. Phys. **21**, 1304 (1950).
[12] L. F. Mattheiss, Phys. Rev. **139**, A1893 (1965).
[13] L. F. Mattheiss, Phys. Rev. **151**, 450 (1966).

energy-band structure have been utilized in the equation derived based on the modified potential model.

It is found that the periodicity deviation from the Schottky line obtained from the above analysis is in very good agreement with the experimental results both in the amplitude and in the phase.

Since the band structures for molybdenum and tantalum have not been disclosed, the values of W_a for them are found by matching the theoretical periodic deviation from the Schottky line with experimental results. The values of W_a for tantalium and molybdenum are found to be 5.23 and 5.44 eV, respectively. Since the work function $\theta=4.19$ eV for tantalum and $\theta=4.3$ eV for molybdenum, it is clear that the Fermi level is 1.04 eV above the bottom of the conduction band for tantalum and 1.14 eV for molybdenum. A calculation has been made to show that these values are unique.

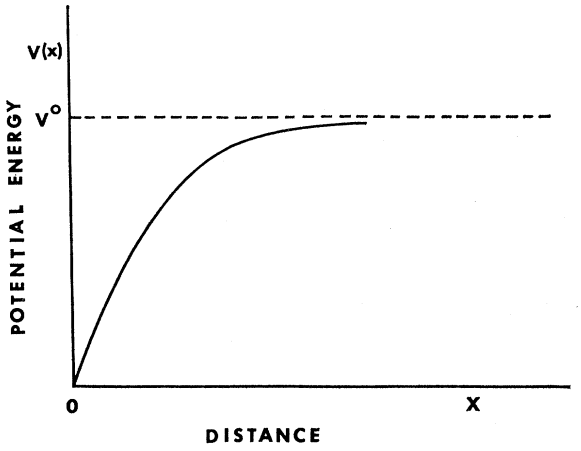

FIG. 1. Model of the surface potential barrier for a metal without an external applied field.

II. ANALYTICAL MODEL FOR SURFACE POTENTIAL BARRIER

When an electron is a great distance from the surface of a metal, the dominant long-range force exerted on it is due to the induced mirror-image charge on the metal. However, within a distance of a few angstroms from the surface, the short-range potential fields that the electron encounters can no longer be represented by the classical image force. Bardeen[10] has made the most rigorous quantum treatment, and the qualitative features of his results have general application. By including exchange and correlation effects, Bardeen[10] found a one-dimensional effective potential asymptotic to the image potential at great distance outside the surface and approaching a constant value inside the metal. Herring and Nichols[4] have discussed the general behavior of an effective one-dimensional potential based on general quantum-mechanical considerations and the results of Bardeen's Hartree-Fock calculation[10] of the charge density in the double layer at the surface of a monovalent metal as follows (Fig. 1): (1) The barrier at the surface is due largely to the exchange and correlation forces, rather than to ordinary electrostatic forces. (2) The potential difference V^0 between a point outside the surface and a point in the interior can be described as

V^0=Fermi energy + work function − (exchange and correlation energies in the interior).

(3) The exchange and correlation potentials decrease as the distance increases (outside the surface) and approach the classical image potential at a large distance from the surface.

Sachs and Dexter[11] treated an approximate quantum-mechanical correction to the classical image-force interaction energy. They obtained a correction term ΔE which gives the order-of-magnitude deviation from the classical image formula due to purely quantum-mechanical effects in the metal. This first-order correction of the interaction energy is inversely proportional to x^2, where x is the distance of the electron from the metal surface.

In order to have a finite value for $V(x)$ at $x=0$, a modified model developed by Seitz[14] is used. For simplicity, an atomic unit is introduced. Thus, the potential barrier model can be written as follows:

$$V(x)=0 \quad \text{for } x\leq 0, \tag{1}$$

$$V(x)=V^0-\frac{1}{2(x+1/2W_a)}+\frac{b}{(x+1/2W_a)^2}-\frac{x}{2(x_0+1/2W_a)^2} \quad \text{for } x>0. \tag{2}$$

The second term of Eq. (2) represents the classical image-force energy; the third term represents the exchange and correlation energies; the last term is the external applied energy. W_a is the summation of Fermi energy E_F and work function θ. $x_0+1/2W_a$ is the position of the maximum of the potential barrier. b is the coefficient of the exchange and correlation energies, depending on the properties of the metal. For $V(0)=0$, we obtain $V^0=W_a-4bW_a^2$.

Figure 2 is the potential-barrier model [expressed as Eqs. (1) and (2)] that will be used in this investigation.

III. DERIVATION OF TRANSMISSION COEFFICIENT

With the potential barrier chosen in Sec. II, the Schrödinger equations are

$$\frac{d^2\psi_I}{dx^2}+W\psi_I=0 \quad \text{for } x\leq 0, \tag{3}$$

[14] F. Seitz, *Modern Theory of Solids* (McGraw-Hill, New York, 1940).

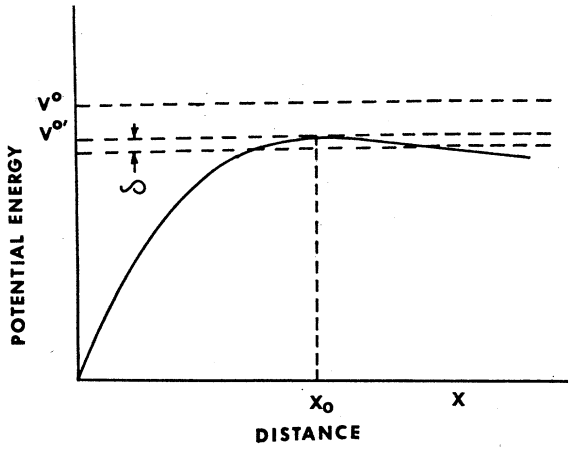

FIG. 2. Model of the surface potential barrier for a metal with an external applied field.

$$\frac{d^2\psi_{II}}{dx^2}+\left(W-W_a+4bW_a{}^2+\frac{1}{2(x+1/2W_a)}-\frac{b}{(x+1/2W_a)^2}+\frac{x}{2(x_0+1/2W_a)^2}\right)\psi_{II}=0 \quad \text{for } x>0, \quad (4)$$

where W is the total energy of the electron.

The solution of Eq. (3) is then

$$\psi_I=a_1e^{iW^{1/2}[x+(1/2W_a)]}+a_2e^{-iW^{1/2}[x+(1/2W_a)]} \text{ for } x\leq 0, \quad (5)$$

where the two exponentials represent the incident and the reflected waves, respectively.

By the WKB approximation, the solution of Eq. (4) is obtained as

$$\psi_{II}=b_1\phi^{-1/4}\exp\left(i\int\phi^{1/2}dx\right)+b_2\phi^{-1/4}\exp\left(-i\int\phi^{1/2}dx\right) \quad \text{for } 0<x<x_0, \quad (6)$$

where

$$\phi=W-W_a+4bW_a{}^2+\frac{1}{2(x+1/2W_a)}-\frac{b}{(x+1/2W_a)^2}+\frac{x}{2(x_0+1/2W_a)^2}. \quad (7)$$

For $x>x_0$, we would like to have a transmitted wave only, i.e.,

$$\psi_{III}=c\phi^{-1/4}\exp\left(i\int\phi^{1/2}dx\right). \quad (8)$$

The constants b_1 and b_2 in Eq. (6) are obtained as follows: Expand the potential function of Eq. (4) as a Taylor series about x_0 and neglecting the higher-order terms. Equation (4) thus becomes a parabolic-cylinder equation:

$$\frac{d^2\psi_{II}}{dx^2}+\left(\alpha+\frac{z^2}{4}\right)\psi_{II}=0, \quad (9)$$

where

$$z=\left(\frac{2}{(x_0+1/2W_a)^3}\right)^{1/4}(x-x_0),$$

$$\alpha=\left[\tfrac{1}{2}(x_0+1/2W_a)^2\right]^{1/2}\epsilon,$$

$$\epsilon=W-W_a+4bW_a{}^2+\frac{1}{x_0+1/2W_a}-\frac{b}{(x_0+1/2W_a)^2}.$$

Solving the above parabolic-cylinder equation (9) and requiring the solution to satisfy condition (8), and comparing the solution to Eq. (6), one obtains the following relations:

$$b_1=e^{-i\pi/8}e^{-\pi\alpha/4}(2\pi)^{1/2}/\Gamma(\tfrac{1}{2}+i\alpha), \quad (10)$$

$$b_2=e^{i3\pi/8}e^{-3\pi\alpha/4}, \quad (11)$$

By utilizing b_1 and b_2 in Eq. (6) and by introducing the boundary conditions

$$\psi_I=\psi_{II} \quad \text{at } x=0, \quad (12)$$

$$\frac{d\psi_I}{dx}=\frac{d\psi_{II}}{dx} \quad \text{at } x=0, \quad (13)$$

the transmission coefficient at the external field E can be obtained from Eqs. (5) and (6):

$$D(E,\epsilon)=1-|a_2/a_1|^2=\left\{1+e^{-2\pi\alpha}+\frac{1}{32}\frac{\phi'^2}{\phi^3}e^{-2\pi\alpha}+\frac{1}{64}\frac{\phi'^2}{\phi^3}-\frac{\phi'}{4\phi^{3/2}}e^{-\pi\alpha}(1+e^{-2\pi\alpha})^{1/2}\left(1+\frac{\phi'^2}{64\phi^3}\right)^{1/2}\times\cos\left[2\int_{x_0}^{x}\phi^{1/2}dx-\arg\Gamma(\tfrac{1}{2}+i\alpha)+\tan^{-1}\frac{\phi'}{8\phi^{3/2}}\right]\right\}^{-1}, \quad (14)$$

where

$$\phi'=\left(\frac{d\phi}{dx}\right) \quad \text{at } x=0, \quad \phi=\phi \quad \text{at } x=0.$$

Equation (14) can be expanded as

$$D(E,\epsilon)=\frac{1}{1+e^{-2\pi\alpha}}-\frac{\phi'^2}{64\phi^3}\frac{1}{(1+e^{-2\pi\alpha})^2}+\frac{\phi'}{4\phi^{3/2}}\frac{e^{-\pi\alpha}(1+\phi'^2/64\phi^3)^{1/2}}{(1+e^{-2\pi\alpha})^{3/2}}\times\cos\left[2\int_{x_0}^{x}\phi^{1/2}dx-\arg\Gamma(\tfrac{1}{2}+i\alpha)+\tan^{-1}\frac{\phi'}{8\phi^{3/2}}\right]+\frac{\phi'^2}{32\phi^3}\frac{e^{-2\pi\alpha}}{(1+e^{-2\pi\alpha})^2}\left(1+\frac{\phi'^2}{64\phi^3}\right)\cos\left[4\int_{x_0}^{x}\phi^{1/2}dx-2\arg\Gamma(\tfrac{1}{2}+i\alpha)+\tan^{-1}\frac{\phi'}{4\phi^{3/2}}\right]. \quad (15)$$

The coefficient of

$$\cos\left(4\int_{x_0}^{x}\phi^{1/2}dx\right)$$

is already very small when $\alpha=0$, and goes rapidly to zero as α is increased. Hence, only a very small error is made by neglecting this term. Since x_0 is of the order of 10^2, the term

$$e^{-\pi\alpha}=\exp\{-\pi[\tfrac{1}{2}(x_0+1/2W_a)^3]^{1/2}\epsilon\}$$

may be neglected except for very small ϵ, i.e., $W\approx V^0$. It follows from Eq. (7) that one obtains

$$\frac{\phi'}{4\phi^{3/2}}=-\tfrac{1}{2}W_a{}^{1/2}\frac{(1-8bW_a)}{(1-4bW_a)^{3/2}} \quad (16)$$

and for a small value of α

$$\arg\Gamma(\tfrac{1}{2}+i\alpha)\sim-(\gamma+2\ln 2)\alpha, \quad (17)$$

where γ is Euler's constant and is equal to 0.5772. Also,

$$\int_{x_0}^{0}\phi^{1/2}(x,\epsilon)dx=\int_{x_0}^{0}\phi^{1/2}(x,0)dx+f(\epsilon).$$

Performing the integration of the left-hand member numerically, one sees that even for the largest ϵ values which need be considered (because of the factor $e^{-\pi\alpha}$ we need consider only very small ϵ values),

$$f(\epsilon)\ll\int_{x_0}^{0}\phi^{1/2}(x,0)dx.$$

Furthermore, $f(\epsilon)$ goes rapidly to zero as $\epsilon\to 0$. Consequently, for the small ϵ values, $f(\epsilon)$ may be neglected. Thus

$$2\int_{x_0}^{0}\phi^{1/2}(x,0)dx=-\tfrac{4}{3}\sqrt{2}\left(x_0+\frac{1}{2W_a}\right)^{1/2}+\frac{2}{W_a{}^{1/2}}-4\sqrt{2}b\left(x_0+\frac{1}{2W_a}\right)^{-1/2}+4bW_a{}^{1/2}. \quad (18)$$

Since $(x_0+1/2W_a)^{1/2}\gg b(x_0+1/2W_a)^{-1/2}$, the third term of Eq. (18) may be neglected compared to the first term. Also, since the exchange and correlation energies approach zero at large distances, we have the following approximate relation:

$$\left(x_0+\frac{1}{2W_a}\right)^{1/2}\approx\left(\frac{1}{2}\left(\frac{e}{E}\right)^{1/2}\right)^{1/2}\approx\left(\frac{3.587\times10^4}{E^{1/2}}\right)^{1/2}.$$

Hence the transmission coefficient is simplified as

$$D(E,\epsilon)=\frac{1}{1+e^{-2\pi\alpha}}-\frac{W_a{}^{1/2}}{2}\frac{(1-4bW_a)}{(1-8bW_a)^{3/2}}\frac{e^{-\pi\alpha}}{(1+e^{-2\pi\alpha})^{3/2}}\times\cos[A-(\gamma+2\ln 2)\alpha], \quad (19)$$

where

$$A=\frac{357.1}{E^{1/4}}-\frac{2}{W_a{}^{1/2}}-4bW_a{}^{1/2}+\tan^{-1}\frac{W_a{}^{1/2}}{4}\frac{(1-8bW_a)}{(1-4bW_a)^{3/2}}. \quad (20)$$

Now, we shall sum $D(E,\epsilon)$ over all electron energies and thus obtain the energy-independent transmission coefficient $\bar{D}(E)$ which is a function only of the temperature, the barrier height, the field, and the coefficient of exchange and correlation energies. Since we are interested only in electrons for which $W\sim V^{0\prime}$, where

$$V^{0\prime}=\left(V^0-\frac{1}{X_0+1/2W_a}\right),$$

the Maxwellian energy distribution may be used. Thus

$$\bar{D}(E)=\frac{1}{kT}\int_0^{\infty}D(E,\epsilon)e^{-\epsilon/kT}d\epsilon.$$

Let

$$(1+e^{-2\pi\alpha})^{-3/2}\sim(1-\tfrac{1}{2}e^{-2\pi\alpha})\sum_{n=0}^{\infty}(-1)^n e^{-2n\pi\alpha}.$$

Thus

$$\bar{D}(E)=\frac{1}{kT}\int_0^{\infty}\sum_{n=0}^{\infty}(-1)^n\times\exp\{[-2n\pi(\tfrac{1}{2}(x_0+1/2W_a)^3)^{1/2}+1/kT]\epsilon\}d\epsilon-\frac{W_a{}^{1/2}}{2kT}\frac{(1-8bW_a)}{(1-4bW_a)^{3/2}}\int_0^{\infty}e^{-\pi\alpha}(1-\tfrac{1}{2}e^{-2\pi\alpha})e^{-\epsilon/kT}\times\sum_{n=0}^{\infty}(-1)^n e^{-2n\pi\alpha}\cos(A-(\gamma+2\ln 2)\alpha)d\epsilon. \quad (21)$$

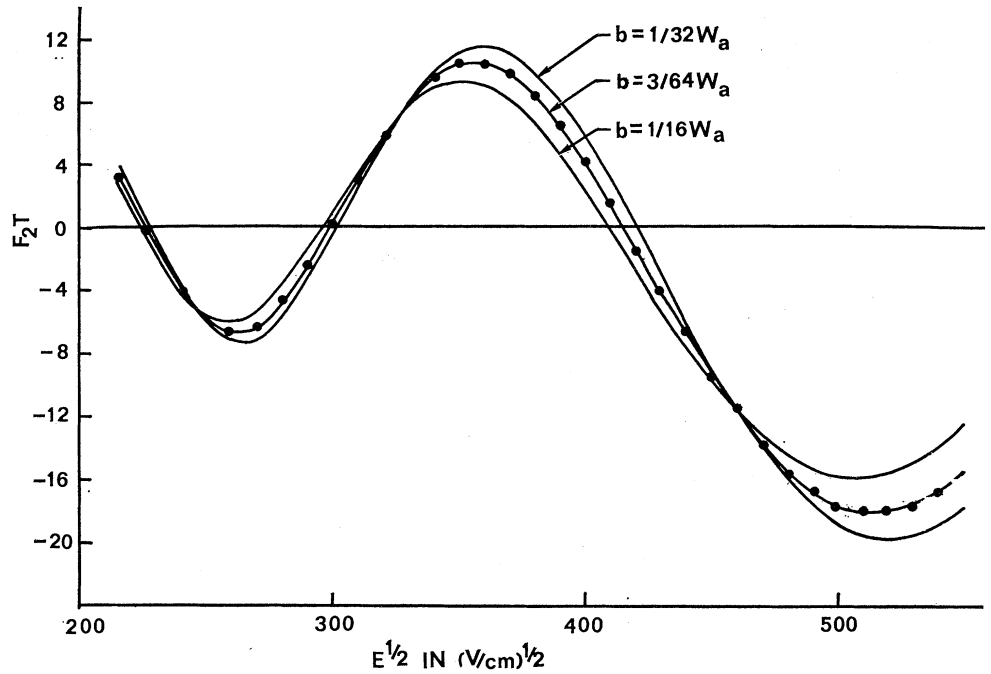

FIG. 3. Thermionic periodic Schottky deviation F_2T as a function of $E^{1/2}$ for tungsten. The dots are the experimental data.

The integration of this expression can be rapidly carried through and leads to a complicated expression. Since for $T\sim1500°\mathrm{K}$, $1/kT$ is negligible compared to $(x_0+1/2W_a)^{3/2}$, to a close approximation

$$\bar{D}(E)=1-\frac{W_a{}^{1/2}}{2kT}\frac{(1-8bW_a)}{(1-4bW_a)^{3/2}}\times[\pi^2+(\gamma+2\ln2)^2]^{-1/2}(\tfrac{1}{2}(x_0+1/2W_a)^3)^{-1/2}\times\cos\left[A-\tan^{-1}\left(\frac{\gamma+2\ln2}{\pi}\right)\right]. \quad (22)$$

The deviations from the Schottky line are then

$$\Delta\log_{10}i=\log_{10}\bar{D}(E)-\log_{10}\bar{D}(0)=F_2',$$

$$F_2'=-\frac{W_a{}^{1/2}}{4.6kT}\frac{(1-8bW_a)}{(1-4bW_a)^{3/2}}[\pi^2+(\gamma+2\ln2)^2]^{-1/2}\times(\tfrac{1}{2}(x_0+1/2W_a)^3)^{-1/2}\cos(A-0.56), \quad (23)$$

where 0.56 in $\cos(A-0.56)$ results from

$$\tan^{-1}[(\gamma+2\ln2)/\pi]=0.56.$$

The current caused by the electrons tunneling through the top of the potential barrier at the metal surface also contributes to the periodic deviation from the Schottky line, increasing the amplitude of deviation. The fields in this region are presumed to be such that the electrons penetrate only the topmost part of the barrier of Fig. 2, i.e., $V^{0\prime}-\delta\leq W\leq V^{0\prime}$. Proceeding as before, we find

$$D'(E,W)=\frac{\exp[-2\pi\alpha'(V^{0\prime}-W)]}{1+\exp[-2\pi\alpha'(V^{0\prime}-W)]}-\tfrac{1}{2}W_a{}^{1/2}\frac{(1-8bW_a)}{(1-4bW_a)^{3/2}}\frac{\exp[-2\pi\alpha'(V^{0\prime}-W)]}{\{1+\exp[-2\pi\alpha'(V^{0\prime}-W)]\}^{3/2}}\times\cos(u), \quad (24)$$

where

$$u=A+(\gamma+2\ln2)\alpha'(V^{0\prime}-W),$$
$$\alpha'=[\tfrac{1}{2}(x_0+1/2W_a)^3]^{1/2}.$$

The energy-independent transmission coefficient resulting from this tunneling term is

$$\bar{D}'(E)=\frac{1}{kT}\int_0^\infty D'(E,\epsilon')e^{-\epsilon'/kT}d\epsilon', \quad (25)$$

where $\epsilon'=V^{0\prime}-W$. Let

$$(1+e^{-2\pi\alpha'\epsilon'})^{-3/2}=(1-\tfrac{1}{2}e^{-2\pi\alpha'\epsilon'})\sum_{n=0}^{\infty}(-1)^n e^{-2n\pi\alpha'\epsilon'}.$$

Substituting Eq. (24) into Eq. (25) and then integrating, we have

$$D'(E)=-\frac{W_a{}^{1/2}}{2kT}\frac{(1-8bW_a)}{(1-4bW_a)^{3/2}}[4\pi^2+(\gamma+2\ln2)^2]^{-1/2}\times(\tfrac{1}{2}(x_0+1/2W_a)^3)^{-1/2}\cos\left(A+\tan^{-1}\frac{\gamma+2\ln2}{2\pi}\right). \quad (26)$$

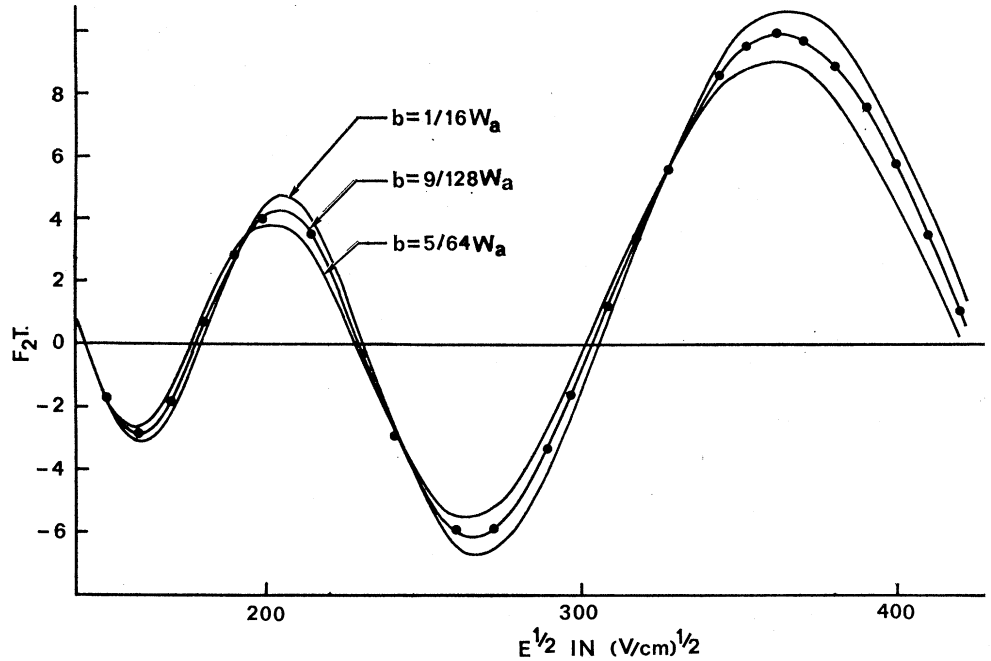

FIG. 4. Thermionic periodic Schottky deviation F_2T as a function of $E^{1/2}$ for rhenium. The dots are the experimental data.

The periodic deviation is then equal to

$$F_2''=\log_{10}\bar{D}'(E)-\log\bar{D}'(0)$$
$$=-\frac{W_a^{1/2}}{4.6kT}\frac{(1-8bW_a)}{(1-4bW_a)^{3/2}}[4\pi^2+(\gamma+2\ln 2)^2]^{-1/2}$$
$$\times(\tfrac{1}{2}(x_0+1/2W_a)^3)^{-1/2}\cos(A+0.302), \quad (27)$$

where 0.302 in $\cos(A+0.302)$ results from

$$\tan^{-1}[(\gamma+2\ln 2)/2\pi]=0.302.$$

Adding Eqs. (23) and (27), we have the total periodic deviation from the Schottky line:

$$F_2=F_2'+F_2''$$
$$=\left[\frac{0.0122\times10^{-6}W_a^{1/2}}{kT}\right]\frac{(1-8bW_a)}{(1-4bW_a)^{3/2}}E^{3/4}$$
$$\times[\cos(A-0.56)+0.5623\cos(A+0.302)]. \quad (28)$$

IV. RESULTS AND DISCUSSION

The theoretical periodic Schottky deviation has been established in Eq. (28) of Sec. III. The calculations

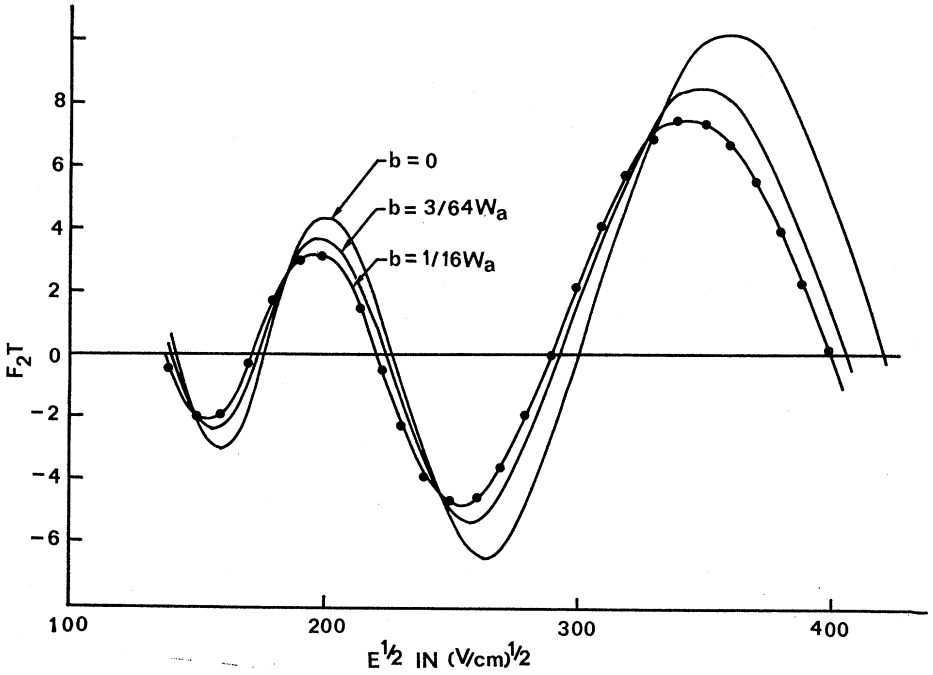

FIG. 5. Thermionic periodic Schottky deviation F_2T as a function of $E^{1/2}$ for molybdenum. The dots are the experimental data.

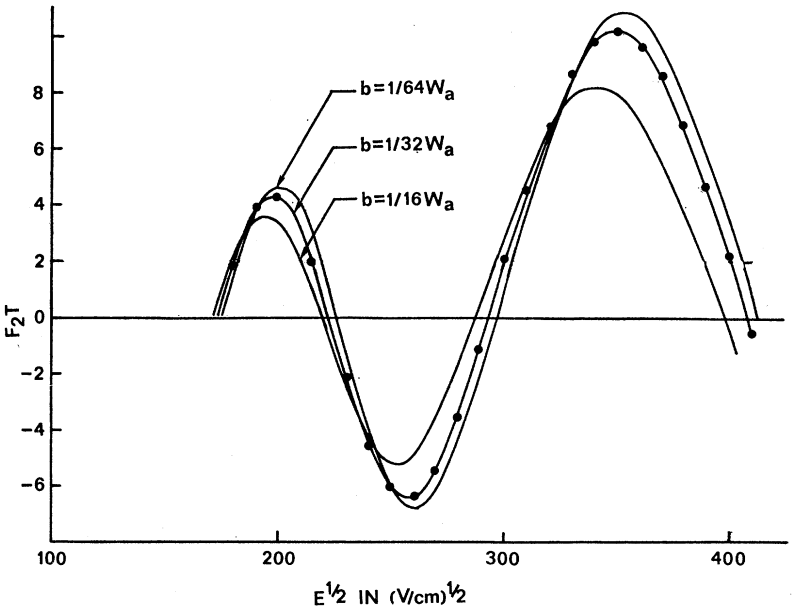

FIG. 6. Thermionic periodic Schottky deviation F_2T as a function of $E^{1/2}$ for tantalum. The dots are the experimental data.

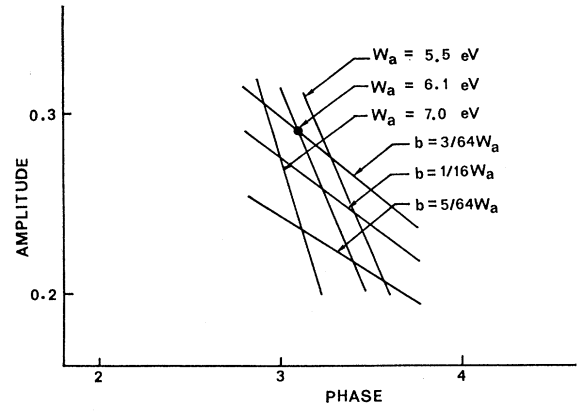

FIG. 7. Amplitude and phase values of Eq. (28) for tungsten with different values of W_a and b.

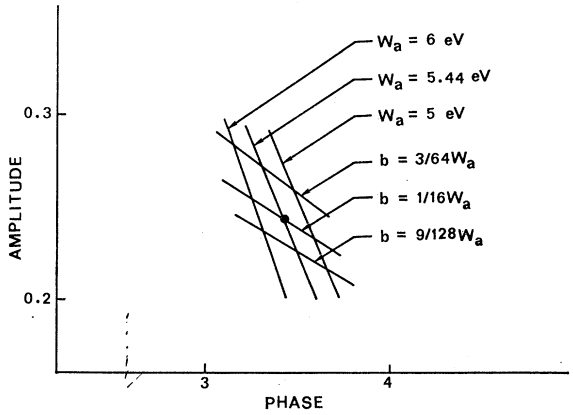

FIG. 9. Amplitude and phase values of Eq. (28) for molybdenum with different values of W_a and b.

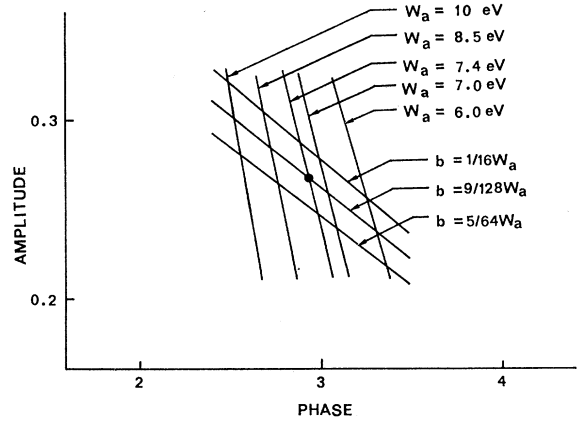

FIG. 8. Amplitude and phase values of Eq. (28) for rhenium with different values of W_a and b.

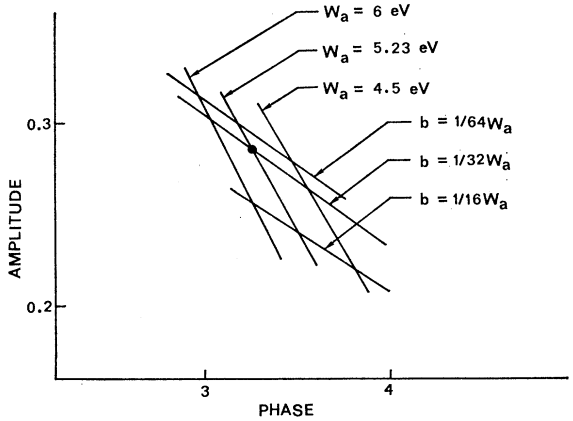

FIG. 10. Amplitude and phase values of Eq. (28) for tantalum with different values of W_a and b.

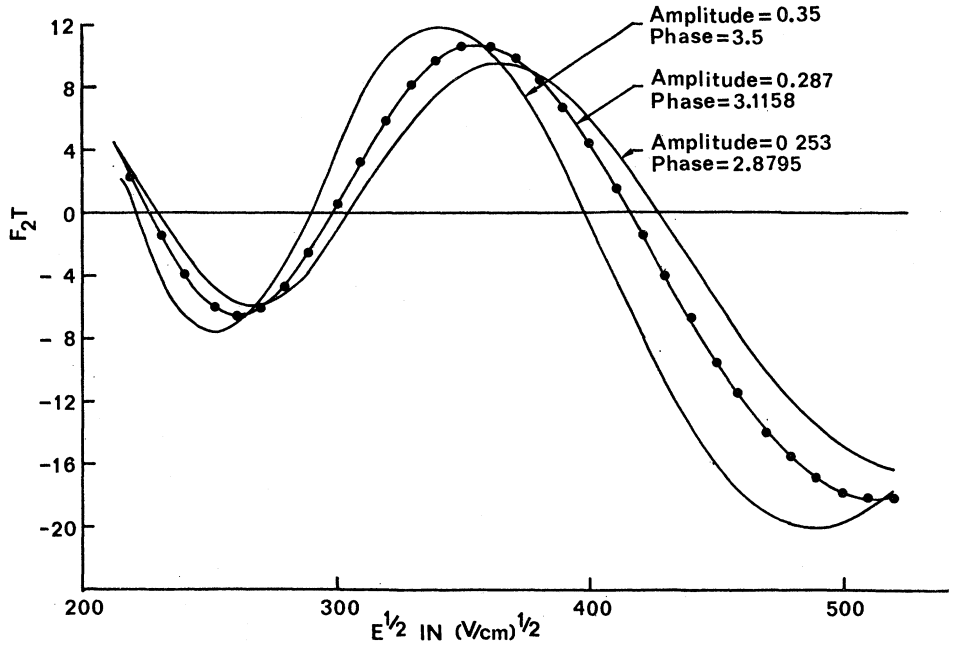

FIG. 11. Thermionic periodic Schottky deviation F_2T of Eq. (28) versus $E^{1/2}$ for tungsten with different amplitude and phase values. The dots are the experimental data.

based on this equation for tungsten, rhenium, molybdenum, and tantalum will now be discussed and compared with the experimental data.

(*1*) *Tungsten.* The experimental data for periodic Schottky deviation for tungsten have been reported by Siefert and Phipps.[2,3] The band-structure calculations have been reported by Mattheiss.[12] Among the various bands that intersect the Fermi surface, the minimum occurs at 0.73 Ry while the Fermi level is at 0.85 Ry. This difference (0.12 Ry) when added to the work function for tungsten which is 4.5 eV = 0.23 Ry, gives us 0.45 Ry for W_a. With this value of W_a substituted into

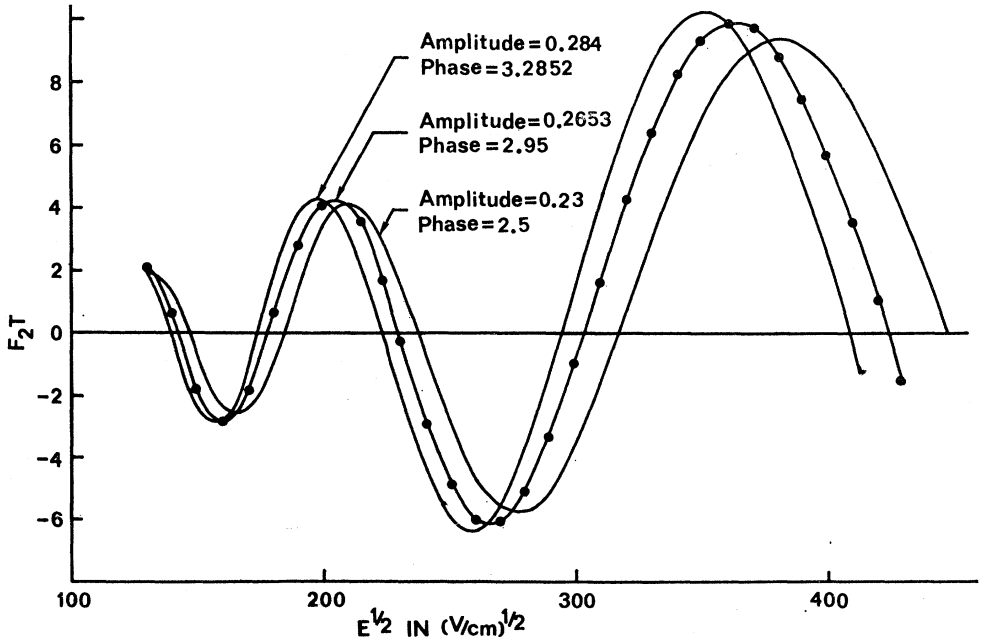

FIG. 12. Thermionic periodic Schottky deviation F_2T of Eq. (28) versus $E^{1/2}$ for rhenium with different amplitude and phase values. The dots are the experimental data.

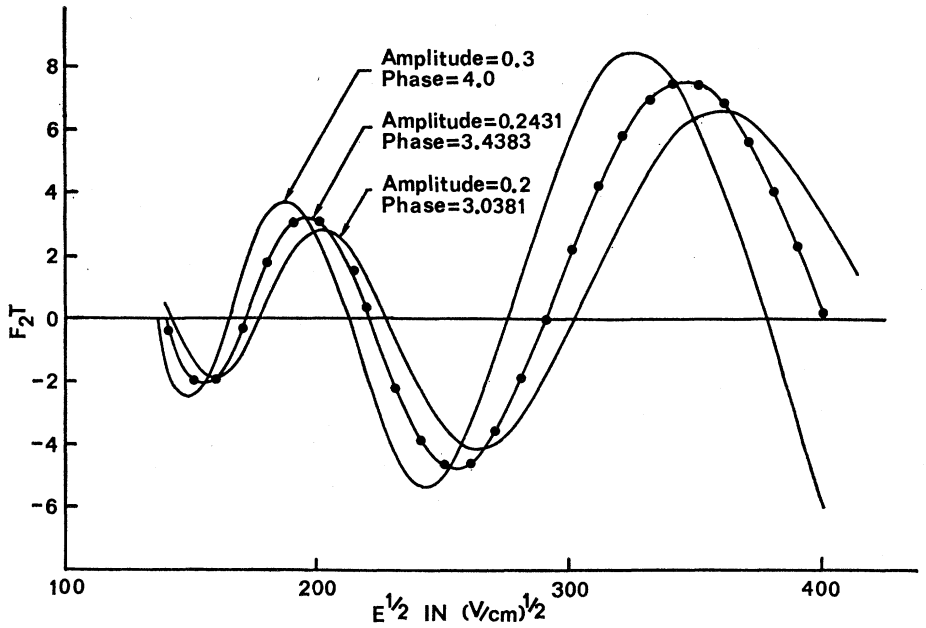

FIG. 13. Thermionic periodic Schottky deviation F_2T of Eq. (28) versus $E^{1/2}$ for molybdenum with different amplitude and phase values. The dots are the experimental data.

Eq. (28) at $T=1600°K$, we obtain the curves for three different exchange and correlation coefficients in Fig. 3. The experimental curve is also plotted in the same figure. A good agreement between theory and experiment can be seen in Fig. 3 when the exchange and correlation coefficient is chosen to be $3/64W_a$.

(*2*) *Rhenium.* A similar procedure is applied to rhenium. The energy-band structure has been calculated by Matteiss.[13] The Fermi energy lies at 0.825 Ry. The lowest value of the highest conduction-band minimum occurs at 0.64 Ry. Using a value of 4.9 eV=0.355 Ry for the work function, the surface barrier potential W_a is 0.54 Ry. This value of W_a substituted into Eq. (28) gives the calculated curves for three different exchange and correlation coefficients at $T=1880°K$ in Fig. 4. These curves are compared with the experimental curve of D'Haenens and Coomes,[15] and a good agreement is noticeable in Fig. 4 when the exchange and correlation coefficient is $9/128W_a$.

(*3*) *Molybdenum.* Since band-structure calculations

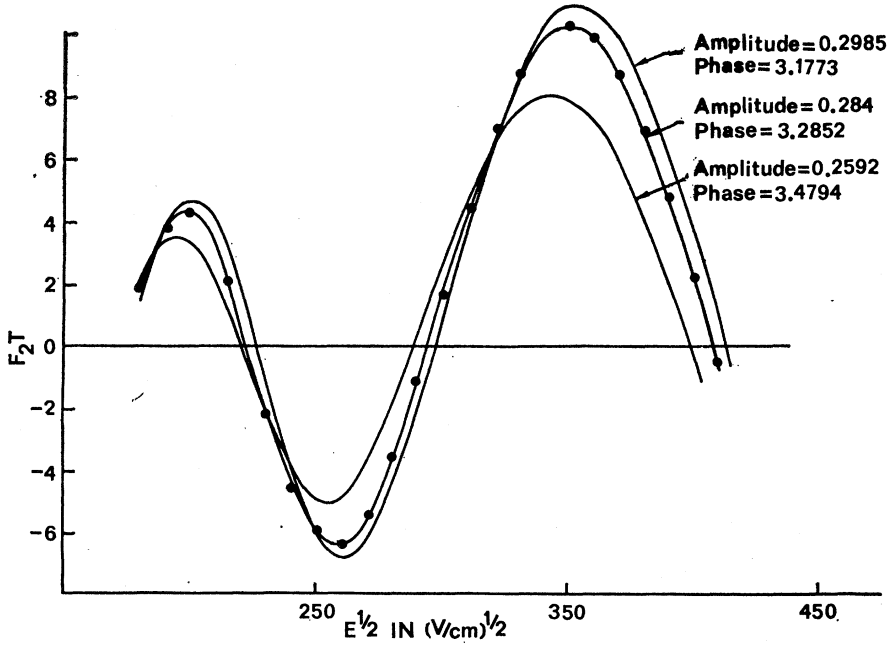

FIG. 14. Thermionic periodic Schottky deviation F_2T of Eq. (28) versus $E^{1/2}$ for tantalum with different amplitude and phase values. The dots are the experimental data.

[15] I. J. D'Haenens and E. A. Coomes, Phys. Rev. Letters 17, 516 (1966).

TABLE I. The values of W_a, b, ϕ, and E_F-E_c for tungsten, rhenium, molybdenum, and tantalum.

	W_a (eV)	b	ϕ (eV)	E_F-E_c (eV)
W	6.1	$3/64W_a$	4.5	1.6
Re	7.4	$9/128W_a$	4.9	2.5
Mo	5.44	$1/16W_a$	4.3	1.14
Ta	5.23	$1/32W_a$	4.19	1.04

are not available for molybdenum, while an experimental curve is available,[16,17] it was decided to obtain W_a by varying its value and the value of the exchange and correlation coefficient until the close agreement in both amplitude and phase was obtained between the theoretical and experimental curves as shown in Fig. 5. The value of W_a corresponding to this theoretical curve is 5.44 eV. Since the work function of molybdenum is 4.3 eV, we can infer that the highest conduction-band minimum occurs in molybdenum at approximately 1.14 eV below the Fermi level. This value of W_a substituted into Eq. (28) at $T=1600°K$ gives the calculated curves for three different exchange and correlation coefficient in Fig. 5; the experimental curve is also plotted in the same figure. A close agreement between theory and experiment can be seen in Fig. 5 when the exchange and correlation coefficient is $1/16W_a$.

(4) *Tantalum.* Again there is no band structure of tantalum available now. The above method in determining the W_a for molybdenum is also applied to tantalum. W_a is found to be 5.23 eV, and $b=1/32W_a$. Since the work function of tantalum is 4.19 eV, we know that $E_F-E_c=1.04$ eV. With the value of $W_a=5.23$ eV substituted into Eq. (28) at $T=1500°K$, we obtain the curves for three different exchange and correlation coefficients in Fig. 6. The experimental data[18,19] are also plotted in the same figure. When the exchange and correlation coefficient is $1/32W_a$, the results obtained in this calculation agree closely with experimental data, as can be seen from Fig. 6.

Briefly, the values of W_a and b can be determined by matching the theoretical equation with the experimental data. The next step is showing that the solution of W_a and b is unique.

From Eq. (28), we find that

$$\text{amplitude}\sim\tfrac{1}{2}W_a^{1/2}\frac{(1-8bW_a)}{(1-4bW_a)^{3/2}},$$

$$\text{phase}\sim\frac{2}{W_a^{1/2}}+4bW_a^{1/2}-\tan^{-1}\frac{W_a^{1/2}}{4}\frac{(1-8bW_a)}{(1-4bW_a)^{3/2}}.$$

The dependence of the amplitude and phase on the W_a and b, expressed by the above equations, is helpful in explaining the uniqueness of the solution. Figure 7 shows the relationship between amplitude and phase for different values of W_a and b for tungsten. There is only one set of amplitude and phase which can match the experimental results. As can be seen clearly in Fig. 7, the values of W_a and b have to be 6.1 eV and $3/64W_a$, respectively.

Similar relationships between amplitude and phase for rhenium, molybdenum and tantalum at different values of W_a and b are plotted in Figs. 8–10. The correct values of amplitude and phase are indicated by small dots in the same figures. Table I summarizes the results of W_a and b for these four elements.

The uniqueness of W_a and b can also be proved in a simple manner. If we plot the periodic Schottky deviation F_2T versus the square root of electric field E, we obtain Figs. 11–14. It is clear that the experimental results agree closely with the theoretical curves which are obtained by using the correct values of W_a and b.

The values of b so obtained fell within the range $0<b<1/8W_a$ which was predicted by Cutler and Gibbons.[9]

[16] G. A. Hass and E. A. Coomes, Phys. Rev. **100**, 640 (1955).
[17] E. G. Brock, A. L. Houde, and E. A. Coomes, Phys. Rev. **89**, 851 (1953).
[18] D. Turnbull and T. E. Phipps, Phys. Rev. **56**, 663 (1939).
[19] R. J. Munick, W. B. La Berge, and E. A. Coomes, Phys. Rev. **80**, 887 (1950).